Activated CaMKIIδ translocates to the RyR nanodomain in cardiomyocytes

Anna Bergan-Dahl[1], Cathrine R. Carlson[1], Martin Laasmaa[1,2], Hariharan Subramanian[3], Adelle Basson[1], Jia Li[1], Almira Hasic[1], Marianne Lunde[1], Hege Ugland[1], Ornella Manfra[1], Enno Klussmann[4, 5], Julie Bossuyt[6], Donald M. Bers[6], Viacheslav O. Nikolaev[3,5], William E. Louch[1,7,*], and Xin Shen[1,7, 8;*]

[1] Institute for Experimental Medical Research, Oslo University Hospital and University of Oslo, NO-0424 Oslo, Norway

[2] Laboratory of Systems Biology, Department of Cybernetics, School of Science, Tallinn University of Technology, Tallinn, Estonia

[3] The University Medical Center Hamburg-Eppendorf, Hamburg, Germany

[4] Max-Delbrück-Centre for Molecular Medicine in the Helmholtz Association (MDC), Berlin, Germany

[5] German Centre for Cardiovascular Research (DZHK), Partner Site Berlin, Germany

[6] Department of Pharmacology, University of California, Davis, CA, USA

[7] K.G. Jebsen Centre for Cardiac Research, University of Oslo, Oslo Norway

[8] Faculty of Medical and Health Sciences, The University of Auckland, Auckland, New Zealand

Running title: Translocation of activated CaMKIIδ to RyRs

Manuscript category: Original article

Word count: 8835

* Corresponding authors:

Xin Shen, email: xin.shen@auckland.ac.nz

Department of Physiology, The University of Auckland, NZ

William E. Louch, email: w.e.louch@medisin.uio.no
Institute for Experimental Medical Research (IEMR), Oslo University Hospital, Ullevål
PB 4956 Nydalen, NO-0424 Oslo, Norway

ABSTRACT

Background: The heartbeat is triggered by the coordinated release of Ca^{2+} from the ryanodine receptor type-2 (RyR) in cardiomyocytes. Phosphorylation of RyR by Ca^{2+}/calmodulin-dependent kinase IIδ (CaMKIIδ) fine-tunes this process in health, while hyperphosphorylation causes excessive, pathological Ca^{2+} release. We investigated how CaMKIIδ is spatially recruited and anchored to RyRs to achieve this functional regulation.

Methods: We employed confocal and dSTORM microscopy to investigate the macro- and nanoscale distribution of CaMKIIδ across cardiomyocytes, respectively. We linked positional rearrangement of the kinase during β-adrenergic stimulation (isoproterenol, Iso) to alterations in RyR phosphorylation and function (Ca^{2+} sparks), and the requirement of the CaMKIIδ anchoring protein AKAP18δ by knockdown/knockout.

Results: Confocal microscopy revealed that macroscale CaMKIIδ localization was not markedly altered during Iso treatment, although a narrowing of its distribution around the Z-lines occurred, where the RyR reside. Higher resolution dSTORM imaging confirmed that local mobilization of CaMKIIδ by Iso decreased the distance from Z-lines and RyRs to the nearest CaMKIIδ by 28% and 12%, respectively. Functionally, kinase translocation into the RyR nanodomain was accompanied by increased channel phosphorylation and Ca^{2+} spark frequency. These actions were dependent on CaMKIIδ activity, since kinase translocation, RyR phosphorylation, and activation were all mimicked by the upstream activator of CaMKIIδ (8-CPT) and prevented by direct CaMKIIδ inhibitors (AIP, N1 peptide). A critical role of AKAP18δ in this mechanism was supported by immunoprecipitation experiments, which showed greater kinase binding to AKAP18δ during Iso stimulation. Furthermore, loss of AKAP18δ by viral-mediated AKAP18δ knockdown or knockout prevented CaMKIIδ translocation to Z-lines. Microtubular disruption also blocked CaMKIIδ translocation.

Conclusions: Collectively, our results indicate that nanoscale movement of CaMKIIδ is closely associated with RyR activation following β-adrenergic stimulation. This translocation depends on an intact microtubular network and kinase binding to AKAP18δ.

Translational implications:

CaMKIIδ-driven phosphorylation of RyRs has emerged as an important driver of aberrant Ca^{2+} homeostasis linked to heart failure and triggered arrhythmias. Understanding and countering the channel's overactivity will require greater insight into how CaMKIIδ is anchored and regulated at the RyR nanodomain. In this work, we demonstrate that RyR phosphorylation during CaMKIIδ activation is accompanied by nanoscale translocation of CaMKIIδ towards the RyRs. We further show that this translocation is dependent on an intact microtubular network and AKAP18δ; a critical CaMKIIδ anchor. These data thus identify AKAP18δ and nanoscale positioning of CaMKIIδ as potential novel therapeutic targets in cardiac disease.

LIST OF ABBREVIATIONS

8-CPT	8-CPT-cAMP
AIP	Autocamtide-2-related Inhibitory Peptide
AKAP	A-kinase anchoring protein
AKAP18	A-kinase anchoring protein 18
AKAP18-KD	A-kinase anchoring protein 18 knock-down
AKAP18-KO	A-kinase anchoring protein 18 γ/δ knockout
AKAP18δ	A-kinase anchoring protein 18δ
CaM	Calmodulin
CaMKII	Ca^{2+}/calmodulin-dependent kinase II
CaMKIIδ	Ca^{2+}/calmodulin-dependent kinase IIδ
Col	Colchicine
dSTORM	Direct stochastic optical reconstruction microscopy
Epac	Exchange protein activated by cAMP
Epac2	Exchange protein activated by cAMP 2

FWHM	Full width at half maximum
Iso	Isoproterenol
LTCC	L-type calcium channels
NND	Nearest-Neighbour Distance
Noc	Nocodazole
PKA	Protein kinase A
PKG	Protein kinase G
PLN	Phospholamban
RyR	Ryanodine Receptor 2
SERCA2	Sarco/endoplasmic Reticulum Ca^{2+}-ATPase 2
SR	Sarcoplasmic reticulum
β-AR	β-adrenergic receptor

1. INTRODUCTION

In cardiomyocytes, the opening of voltage-gated L-type calcium channels (LTCCs) during the action potential enables Ca^{2+} entry, which in turn triggers a larger release of Ca^{2+} via ryanodine receptors type-2 (RyRs) in the sarcoplasmic reticulum (SR) membrane. The binding of released Ca^{2+} to troponin C in the myofilaments elicits myocyte contraction. Relaxation is mediated mainly by the SR Ca^{2+} ATPase 2 (SERCA2), which recycles Ca^{2+} back into the SR; an action that is regulated by SERCA2's endogenous inhibitor, phospholamban (PLN)[1,2].

Beat-to-beat Ca^{2+} cycling is fine-tuned by auxiliary proteins, such as Ca^{2+}/calmodulin-dependent protein kinase IIδ (CaMKIIδ)[3]. Each CaMKIIδ monomer consists of a C-terminal association domain, a regulatory domain, and an N-terminal catalytic domain. When the kinase is inactive, the regulatory domain binds directly to the T-site and the S-site in the catalytic unit, keeping the kinase in a "closed" autoinhibited conformation[4,5]. During activation, Ca^{2+}/CaM binds to the regulatory domain and displaces it from the T- and S-site. The kinase then takes on an "open" conformation which allows it to phosphorylate target proteins, including LTCCs, RyRs, and PLN, and modify these proteins' activities[3,5,6]. For example, CaMKIIδ phosphorylates RyR at Serine 2814; a modification that results in increased Ca^{2+} sensitivity and a lowered activation threshold[7,8]. In cardiovascular diseases such as heart failure, CaMKIIδ overactivity drives

excessive RyR Ca^{2+} leak[9,10] and dispersion of channel clusters[11,12]. These changes are, in turn, linked to the generation of cardiac arrhythmias[13,14] and weakened contraction[11,15].

While the importance of CaMKIIδ activity in healthy and diseased hearts is well characterized[3,6], less is known about how the kinase reaches its targets. We recently discovered that AKAP18δ, an A-kinase anchoring protein, anchors CaMKIIδ to nearby PLN and RyR to enable the phosphorylation of these proteins[16]. Importantly, we found that CaMKIIδ activity could be regulated by its binding to distinct domains within AKAP18δ[16]. This raises the question of how CaMKIIδ is spatially recruited to these sites. Previous work performed in neuronal cells has shown that activated CaMKII undergoes translocation to phosphorylate effector proteins[17-19]. Work by Wood *et al.* revealed that CaMKIIδ also exhibits a high degree of mobility in cardiomyocytes[20]. In particular, the authors observed that electrical pacing induced CaMKIIδ translocation away from Z-lines, while reducing intracellular [Ca^{2+}] by chelators, stabilized CaMKIIδ at Z-lines. Thus, it remains unclear how activated CaMKIIδ reaches targets such as RyRs, since the majority of these channels are located near Z-lines[21].

We presently hypothesized that activation of CaMKIIδ promotes its translocation to RyRs in an AKAP18δ-dependent manner. Employing dSTORM super-resolution microscopy, we found that CaMKIIδ exhibited preferential Z-line localisation at baseline and exhibited a nanoscale translocation toward the RyR nanodomain upon β-adrenergic stimulation. This translocation was accompanied by an increase in RyR phosphorylation and Ca^{2+} spark frequency and was blocked by CaMKIIδ inhibitors. Moreover, CaMKIIδ translocation was observed to require an intact microtubule network and AKAP18δ, suggesting a mechanism by which physical displacement of the activated kinase enables RyR phosphorylation.

2. MATERIALS AND METHODS

Please see the extended Materials and Methods section in the Supplementary Material for a detailed description of the methodology.

2.1 Animal use and ethical approval

All animal experiments were performed with approval from the Norwegian Food Safety Authorities (approvals no. 15889, 20208, 30114), the equivalent German authority (local authority: Freie und Hansestad Hamburg Behörde für Justiz, approval no. N066/2000), and the UC Davis Institutional Animal Care and Use Committee. These approvals are in accordance with the Guide for the Care and Use of Laboratory Animals (NIH publication no. 85-23, revised 2011) and Directive 2010/63/EU of the European Parliament.

All research animals were housed in a temperature- and humidity- controlled facility on a 12 h: 12 h light-dark cycle with *ad libitum* access to food and water. For cardiomyocyte isolation, animals were anesthetized by continuous inhalation of 5% isoflurane and 95% O_2 and sacrificed by excision of the heart (rats and rabbits) or cervical dislocation (mice).

3. RESULTS

3.1 β-adrenergic stimulation causes CaMKIIδ translocation to RyRs at the Z-lines

We first investigated the relative positioning of CaMKIIδ and RyRs under baseline conditions in left ventricular rat cardiomyocytes using confocal microscopy (Figure 1a). We observed marked colocalization of these proteins, with a striated pattern consistent with preferential localization at the Z-lines. Indeed, co-staining of α-actinin and CaMKIIδ confirmed this arrangement (Figure 1b). Negative controls performed with secondary antibodies alone showed no such staining pattern (Figure S1).

We next investigated whether the cellular distribution of the kinase is affected by acute treatment with the β-adrenergic agonist Isoproterenol (Iso, 100 nM, 10 min). Confocal imaging revealed no marked changes in the macroscale CaMKIIδ signal relative to Z-lines (Figure 1b-c). However, closer examination of CaMKIIδ distribution revealed a narrowing of fluorescent peaks at the Z-lines following Iso treatment, as indicated by fluorescence-intensity profiles (Figure 1d) and measurements of the full width at half maximum (FWHM) of these signals (Figure 1e). Thus, despite the limited resolution of confocal imaging, these observations suggest that CaMKIIδ may translocate closer to Z-lines following Iso treatment.

We used 2-colour dSTORM super resolution microscopy for greater detailed resolution of CaMKIIδ movement in response to Iso. In agreement with our confocal imaging, dSTORM imaging revealed a shift of CaMKIIδ positions towards α-actinin following Iso treatment (Figure 1f). Specifically, quantification of the nearest-neighbour-distance (NND) from α-actinin to the closest CaMKIIδ confirmed a significant decrease in these values by 28% (± SEM 6%) following 10 min of Iso treatment (Figure 1g). On the other hand, large-scale, cell-wide movements of CaMKIIδ were not apparent (Figure 1h) in both the presence and absence of Iso. Here we observed that ~27% of all CaMKIIδ clusters remained within 50 nm of α-actinin, while remaining clusters were found at relatively random longitudinal distances along the half-sarcomere. The same was true for overall CaMKIIδ area (Figure S2a), except that roughly half of the total CaMKIIδ area was within that 50 nm of α-actinin, indicating that the Z-line CaMKIIδ clusters are larger on average than those elsewhere. These results were also confirmed in rabbit cardiomyocytes, where a strong tendency of translocation towards the Z-lines was observed following Iso treatment, without alterations to the macroscale distribution or area of CaMKIIδ (Figures S3a-d).

Similar results were obtained for 2-colour dSTORM imaging of RyR and CaMKIIδ (Figure 1i) as Iso application reduced the distance from the average RyR cluster to the closest CaMKIIδ by 12% (±SEM 2%) (Figure 1j). The overall macroscale distribution of CaMKIIδ clusters again remained largely unchanged (Figure 1k) with over half of the CaMKIIδ within 150 nm of an RyR cluster. Furthermore, when we assessed the colocalization of CaMKIIδ-RyR by a proximity ligation assay, we found a 36% (± SEM 5%) increase in the colocalization signal following Iso treatment (Figure 1l). Note that this increase in colocalization is unlikely to result from changing RyR localisation, since we found no alterations in the nearest α-actinin-RyR distance after Iso treatment (Figure S2b). Notably, we observed that the nanoscale effects of Iso on CaMKIIδ positioning at Z-lines were partially reversible with wash-out (Figure S4a), while the overall distribution of CaMKIIδ across the sarcomere remained unaltered by either Iso or wash-out (Figure S4b).

Taken together, these data support that acute β-adrenergic receptor (β-AR) stimulation promotes nanoscale translocation of CaMKIIδ towards RyRs located near the Z-lines, without affecting the broader arrangement of the kinase across the sarcomere. Notably, this Iso-induced coalescence of

CaMKIIδ at Z-lines in these quiescent cells is opposite to effects induced by electrical pacing of adult ventricular myocytes (Figure S5a, b). This finding is in agreement with a previous confocal study in adult rabbit ventricular myocytes, where pacing induced CaMKIIδ mobility and distance from Z-lines (Wood et al)[20]. However, when Iso was applied together with pacing, the CaMKIIδ localization was intermediate (Figure S5a), indicating a competition of influence of Iso vs. pacing on CaMKIIδ localization to the Z-line.

3.2 CaMKIIδ movement is dependent on kinase activation.

Next, we tested whether CaMKIIδ translocation is directly dependent on its activation state. In cardiomyocytes pre-treated with the selective CaMKII inhibitor AIP (Autocamtide-2-related Inhibitory Peptide, myristoylated, 2 μM, 45 min), acute application of Iso no longer resulted in a shift in CaMKIIδ localisation toward Z-lines (Figure 2a-b) or RyRs (Figure 2c-d). Application of another peptide inhibitor of CaMKIIδ called N1 (AKAP18-N (55-74)[16]; with a cell-permeable TAT-tag, 5 μM, 45 min), similarly inhibited Iso-induced translocation of the kinase (Figure S6a-c). Importantly, neither AIP nor N1 had any effect on the overall baseline NND from α-actinin to CaMKIIδ in the absence of Iso stimulation (Figure S6e). On the other hand, activation of CaMKIIδ via the Exchange protein activated by cAMP 2 (Epac2) pathway[33] using 8-CPT-cAMP (8-CPT, 10 μM, 10 min)[33] reproduced effects similar to Iso, inducing nanoscale movement of CaMKIIδ towards the Z-lines (Figure 2a-b) and RyRs (Figure 2c-d). At the macroscale, neither AIP, N1, nor 8-CPT altered the overall CaMKIIδ distribution (Figure 2e, S6d). These results support that nanoscale CaMKIIδ movement toward the RyRs at the Z-lines is dependent on the activity of the kinase.

It is well established that CaMKIIδ activation during β-AR stimulation causes RyR phosphorylation at Ser2814[34], and that the resulting channel activation augments spontaneous Ca^{2+} release events called Ca^{2+} sparks[35]. In our hands, CaMKIIδ translocation towards RyRs coincided with expected alterations in RyR phosphorylation status and activity. Indeed, application of either Iso or 8-CPT significantly increased RyR phosphorylation at Ser2814, whereas AIP (tendency) or N1 treatment attenuated the effect of Iso (Figure 2f, S6f). Functional measurements of Ca^{2+} sparks (Figure 2g, S6g) were closely aligned with these effects, as Iso and 8-CPT treatments led to similar increases in spark frequency and size, while AIP and N1 reversed

the effect of Iso on spark frequency back to control levels and attenuated spark size (Figure 2h-i, S6h-i). These data raise the possibility that activation of RyRs may be induced by nanoscale translocation of CaMKIIδ to the channels.

CaMKIIδ can also be activated by oxidation[36]. To test whether this means of kinase activation has similar effects on its translocation, we exposed cardiomyocytes to H_2O_2 (100μM) for 15 min. In these cells, no translocation towards Z-lines was observed (Figure S7a), and the broader distribution of the kinase across the sarcomere remained unchanged (Figure S7b). These findings suggest that control of CaMKIIδ positioning is linked to downstream effects of β-AR stimulation, but not necessarily other mechanisms of kinase activation.

3.3 CaMKIIδ anchoring and translocation to the RyR nanodomain is dependent on AKAP18δ

Figure 3a-d shows potential mechanisms by which CaMKIIδ may translocate and functionally regulate RyRs. These mechanisms are likely facilitated by AKAP18δ which we have previously shown to anchor CaMKIIδ at RyR[16]. We thus hypothesized that the observed CaMKIIδ shift toward RyRs following β-AR or 8-CPT activation is mediated by either the movement of AKAP18δ itself (Figure 3a), or by the release of CaMKIIδ from AKAP18δ to RyR (Figure 3b) as CaMKIIδ is known to co-immunoprecipitate with RyR[7,37]. Alternatively, CaMKIIδ could be recruited to RyR-associated AKAP18δ (Figure 3c), or the CaMKIIδ position on the AKAP18δ protein could be shifted closer to the RyR (Figure 3d), given that there are distinct binding sites between CaMKIIδ and AKAP18δ[16].

We began by ruling out the possibility of movement of AKAP18δ itself driving kinase translocation (Figure 3a) since 2-colour dSTORM imaging revealed no shift in the position of AKAP18δ towards the Z-line during Iso treatment (Figure 3e-f). We next tested whether CaMKIIδ is released from AKAP18δ following activation, bringing it closer to its site of action at RyRs (Figure 3b). To test this possibility, we compared the degree of interaction between CaMKIIδ and AKAP18δ before and after β-adrenergic stimulation. Immunoprecipitation analysis revealed that *more* CaMKIIδ co-immunoprecipitated with AKAP18δ following Iso stimulation (Figure 3g), ruling out the release of CaMKIIδ from AKAP18δ (Figure 3b).

An alternative explanation is that activated CaMKIIδ is critically recruited to AKAP18δ (Figure 3c) or that it moves within AKAP18δ (Figure 3d) to allow RyR phosphorylation, both in line with the increased co-immunoprecipitation. To investigate these possibilities, we experimentally reduced AKAP18δ expression by culturing LV cardiomyocytes in the presence of adenovirus carrying a short hairpin sequence for AKAP18. In comparison with cells treated with adenovirus expressing a scrambled control sequence (SCRM), AKAP18 knockdown (AKAP18-KD) significantly reduced AKAP18 mRNA from 72 h following transduction (Figure 4a), with further reduction after 96 h post transduction (Figure 4b-c), where we observed an ~60 % decrease in AKAP18δ expression. Antibody specificity was confirmed by a blocking peptide (Figure S8a).

Based on the above results, we employed cardiomyocytes cultured for 96 h to study effects on CaMKIIδ movement using 2-colour dSTORM. Iso-treatment still induced a marked translocation of CaMKIIδ towards the Z-lines, indicating that the mechanism controlling CaMKIIδ positioning remains intact following cell culture (Figure S8b). We also found no alteration in CaMKIIδ location when comparing scrambled virus treatment to the non-viral control (Figure S8c). However, we observed a markedly smaller α-actinin to CaMKIIδ distance in basal conditions for AKAP18-KD (vs. SCRM control; Figure 4d-e), which may reflect a population of CaMKIIδ that has become associated with an alternative binding partner when AKAP18δ levels are reduced. Furthermore, we demonstrated that the kinase translocation mechanism remained intact in our SCRM cells treated with Iso but was lost in AKAP18-KD cells (Figure 4e). At the macroscale, reduction of AKAP18 did not disrupt the distribution of CaMKIIδ clusters, in the presence or absence of Iso (Figure 4f).

Further evidence for a key role of AKAP18δ in controlling CaMKIIδ translocation was provided by experiments employing AKAP18-knock-out mice (AKAP18-KO). As in viral knockdown experiments, 2-colour dSTORM revealed that Iso-induced CaMKIIδ translocation toward Z-lines was prevented in AKAP18-KO cardiomyocytes (Figure 4g-h). Similarly, neither AKAP18 KO nor Iso had any notable effect on the macroscale distribution of CaMKIIδ clusters (Figure 4i), indicating that AKAP18δ is not the sole anchor for CaMKIIδ along the Z-lines.

Taken together, these findings support a mechanism consistent with those schematically illustrated in Figures 3c or d, where CaMKIIδ movement toward the RyR nanodomain is effected by kinase translocation to AKAP18δ, or switching of its binding sites within AKAP18δ. How can

we distinguish between these two possible mechanisms? We hypothesized that directed CaMKIIδ translocation to AKAP18δ would reduce the variability in RyR-to-CaMKIIδ distances by recruiting CaMKIIδ to a common anchoring point close to RyR, whereas site-switching within AKAP18δ would rather maintain NND variability (depicted in Figure S9a and b, respectively). We found that Iso-treatment reduced the distance variability (Figure S9c), supporting the translocation mechanism displayed in Figure 3c as the most likely explanation.

3.4 AKAP18δ contributes to regulation of basal phosphorylation of RyRs at Ser2814

To examine potential functional consequences of CaMKIIδ translocation, we investigated whether AKAP18-KD would affect CaMKIIδ activity at the RyRs, as indicated by Ser2814 phosphorylation. Under baseline conditions, we observed that reduced AKAP18δ level tended to lower Ser2814 phosphorylation (Figure 4j). However, AKAP18-KD cells still exhibited a significant increase in Ser2814 phosphorylation during Iso treatment, which resembled the response observed in cells treated with scrambled control virus. This finding suggests that while AKAP18δ anchors CaMKIIδ near RyRs, to functionally regulate the channels, alternative mechanisms also facilitate CaMKIIδ-mediated RyR activity during β-adrenergic stimulation.

3.5 Microtubular integrity is necessary for CaMKIIδ translocation

Our results thus far suggest an important anchoring role of AKAP18δ, although the mechanism by which CaMKIIδ reaches/is transported to these anchor sites remains unclear. Previous work in neuronal cells has shown that activated CaMKII may bind to microtubules[38]. To address whether CaMKIIδ movement at the nanoscale could be dependent on the cellular network of microtubules, we disrupted the network using a 2h treatment with either colchicine (Col, 10 μM, 2 h) or nocodazole (Noc, 10 μM, 2 h). Next, we used 2-colour dSTORM imaging to assess effects on CaMKIIδ placement and movement. Neither colchicine (Figure 5a-b) nor nocodazole (Figure 5c-d) altered the basal α-actinin to CaMKIIδ NND compared to untreated control cells. However, the usual Iso-induced reduction in NND from α-actinin to CaMKIIδ was not present when microtubules were destabilized (Figure 5b, d). Analysis of the macroscale distribution of

CaMKIIδ revealed that the overall distribution of CaMKIIδ clusters also remained largely unchanged (Figure 5e-f), as did the broader organization of RyRs and AKAP18δ (Figure S10).

Taken together, these findings suggest that a stable microtubule network is required for nanoscale translocation of activated CaMKIIδ to the Z-lines, although it is unclear whether this happens through direct transport of CaMKIIδ along the microtubules, through binding to microtubule-associated proteins, or via regulatory microtubule effects at dyadic microdomains.

4. DISCUSSION

In this work, we have employed advanced light microscopy techniques to reveal CaMKIIδ translocation within the RyR nanodomain. Specifically, we showed that CaMKIIδ activation via the β-AR or Epac signaling pathways induced kinase movement towards RyRs at the Z-lines. This translocation was prevented by employing CaMKIIδ inhibitors. Functionally, we observed that CaMKIIδ activation and movement were accompanied by augmented RyR phosphorylation at Ser2814 and increased Ca^{2+} spark frequency. Mechanistically, we observed that CaMKIIδ translocation, and likely activity, within the RyR nanodomain was dependent on both its anchoring by AKAP18δ and an intact microtubule network. These data provide new, nanoscale understanding of the dynamic role that CaMKIIδ plays in fine-tuning cardiomyocyte Ca^{2+} release and contractility.

4.1 CaMKIIδ localization at baseline and following activation

CaMKIIδ phosphorylation of RyR at Ser2814[7,37] is expected to require close proximity between the kinase and receptor. Our confocal and dSTORM analysis revealed that the majority of CaMKIIδ is near Z-lines, where RyR localization is most prominent (Figure 1a-c), and that Iso-stimulation leads to CaMKIIδ translocation towards the Z-lines and RyR (Figure 1d-e, g, j). A similar reduction in NND was observed following cellular treatment with the Epac activator 8-CPT-cAMP (Figure 2a-d). Although 8-CPT-cAMP activates PKA and PKG in addition to CaMKIIδ, we observed that treatment with the CaMKIIδ inhibitors AIP and N1 prior to Iso stimulation prevented the CaMKIIδ translocation (Figure 2a-d, S6a-c). These findings support that CaMKIIδ translocation is linked to the kinase's activation state. Interestingly, additional data indicated that the PKA inhibitor H89 (which may also affect other kinases such as PKG) also prevented the effect of Iso on CaMKIIδ translocation (Figure S11a-b). Since PKA is crucial for

mediating an augmentation of Ca^{2+} homeostasis during β-adrenergic stimulation, H89's effects likely reflect decreased activation of CaMKIIδ by Ca^{2+}. However, we noted that direct activation of CaMKIIδ through oxidation with H_2O_2 did not induce translocation (Figure S7), which supports that the manner by which CaMKIIδ is activated is critical. Given that PKA and CaMKIIδ may have overlapping roles in regulating RyR phosphorylation[39], future work should be aimed at unravelling these coordinated functions.

While our findings are novel in cardiomyocytes, previous work in other cells has shown that CaMKIIδ is translocated to its target proteins in an activity-dependent manner, and that this translocation is essential for the targets' phosphorylation[17,40]. Investigations of other kinases have similarly demonstrated that their translocation to membranous compartments precedes phosphorylation of target proteins at these locations[41,42]. Thus, physical recruitment to effector proteins may be a paradigm that is shared among diverse kinases. Notably, while previous work has reported macroscale CaMKII displacement[17,40-42], our findings in cardiomyocytes have shown nanoscale translocation, which may reflect the very tight geometry of the dyad.

4.2 The role of AKAP18δ

The preferential localization of CaMKIIδ near Z-lines, both at baseline and following Iso stimulation (Figure 1a-c) is consistent with its anchoring at these sites. Based on our recent work[16], we hypothesized that AKAP18δ might provide such a role. Although Shannon *et al* reported mobility of AKAP18γ[43], we did not observe alteration in the NND from Z-lines (α-actinin) to AKAP18δ (Figure 3f) following Iso. These results, alongside increased CaMKIIδ co-immunoprecipitation with AKAP18δ after Iso stimulation (Figure 3g), indicated that AKAP18δ serves as a CaMKIIδ anchor at rest, and as a hub that can accommodate additional CaMKIIδ molecules during β-AR stimulation. This mechanism is in line with the mechanism proposed in Figure 3c. Such a role of AKAPs is already well established for the recruitment and anchoring of PKA[44]. Further support for the mechanistic model described in Figure 3c was provided by AKAP18-KD in cultured rat cardiomyocytes. With the caveat that cell culture induces an inevitable rounding of cellular edges and partial loss of t-tubules (Figure S12), we nevertheless observed that AKAP18-KD prevented CaMKIIδ translocation (Figure 4e), as did AKAP18γ/δ-KO (Figure 4h). However, we still noted preferential localization of the kinase at the Z-lines

despite AKAP18δ removal in both KD and KO models (Figure 4f, 4i). This finding suggests that AKAP18δ is not the only anchoring point for CaMKIIδ at the Z-lines, in agreement with previous work showing that CaMKIIδ can be anchored at LTCCs[45], α-KAP[46], and at the RyR complex itself[37]. Thus, a secondary anchoring protein, potentially with a weaker CaMKIIδ affinity than AKAP18δ, may serve as a kinase anchor closer to Z-lines following AKAP18δ reduction. Such a binding site may provide redundancy in the machinery controlling RyR phosphorylation.

Interestingly, the KD and KO models displayed differences in baseline CaMKIIδ positioning (Figure 4e, 4i), which may reflect the presence of a compensatory mechanism in the KO mouse, while there was less time for such adaptation following acute AKAP18 KD. Species differences should also be considered. Notably, the rat heart only expresses the δ variant of AKAP18[47], while the mouse heart expresses the γ and δ isoforms. Both AKAP18γ and δ variants contain an anchoring domain for CaMKIIδ[16] and both were deleted in our knockout mouse model, arguing against an important role of isoform differences between species.

4.3 Alternative mechanisms

The above findings point towards AKAP18δ being important for accepting translocating CaMKIIδ, as illustrated in Figure 3c. However, since previous work by Carlson *et al* has shown that AKAP18δ harbours two distinct binding sites for CaMKIIδ[16], an alternative mechanism could be envisioned where CaMKIIδ moves between these two sites, bringing it closer to RyRs (See Figure 3d). We expect that such site-switching within AKAP18δ would maintain distance variability between CaMKIIδ and RyR (Figure S9a, b). Instead, our measurements showed a decrease in the variability of this NND (Figure S9c), suggesting that there is in fact kinase movement to AKAP18δ binding close to RyRs (Figure 3c, S9a). Prior to its translocation, this population of CaMKIIδ may either be unbound or bound to other anchors more distal from the Z-lines/RyRs. These results are further corroborated by the predicted distance between the two AKAP18δ-binding sites for CaMKIIδ. Using AlphaFold[27,28] and NGL viewer[29,30], we found that the binding sites were separated by less than 10 nm; a distance that is shorter than the one observed for our NND shift in CaMKIIδ (Figure 1g, 1j).

It's also possible that upon CaMKIIδ activation, the kinase does not bind differently to AKAP18δ, but rather changes its conformation to bring it closer to RyRs. A similar mechanism has been reported for AKAP-anchored PKA, as flexibility within the AKAP holoenzyme allows substrate phosphorylation while the kinase remains affixed[48]. In the case of CaMKII, plasticity of the kinase's structure can include a dynamic transition from a compact to an extended conformation[4]. For CaMKIIα, kinase plasticity can include a transition from a compact to an extended conformation in the range of 15 to 35 nm[49]. Although such a transition is in a similar scale as our measured reduction in RyR-CaMKIIδ NND following Iso stimulation, a very low proportion of CaMKIIα has been found to exist in the compact conformation, hence arguing against an importance in our experiments. Furthermore, we expect that alteration of the CaMKIIδ diameter would not alter the variability in RyR-to-CaMKIIδ NND to the extent observed (Figure S9c). The observed reduction in this distance is consistent with greater trafficking of CaMKIIδ to AKAP18δ (Figure 3c), further supported by the increase in CaMKIIδ and AKAP18δ binding following Iso stimulation (Figure 3f).

4.4 Functional implications

Regardless of the precise underlying mechanism, it is highly likely that the provided proximity between AKAP18δ-bound CaMKIIδ and RyRs enables channel phosphorylation. However, our previous work showed that binding of CaMKIIδ to AKAP18δ also lowers the kinase's threshold for Ca^{2+} activation[16]. Thus, AKAP18δ may facilitate RyR phosphorylation not only by positioning CaMKIIδ nearby, but by allowing activation at lower local $[Ca^{2+}]_i$. Although we cannot determine a causative relationship, we certainly observed that Iso-induced CaMKIIδ translocation was paired with marked increases in RyR phosphorylation (Figure 2f) and Ca^{2+} spark frequency (Figure 2g-h). An intriguing possibility is that RyR activity itself, which is a key regulator of CaMKIIδ activation, may contribute to control of kinase positioning, perhaps on a beat-to-beat basis. For example, a positive feedback loop could be envisioned where activated CaMKIIδ is translocated toward Z-line RyRs, and then maintained there following RyR activation, where additional Ca^{2+} release can increase CaMKIIδ activation. Indeed, our preliminary experiments performed with PKA inhibition described above are consistent with such a mechanism of positive feedback from the RyRs (Figure S11). Under more physiological conditions, such as during continuous pacing, Ca^{2+} entry via LTCCs and release by RyRs may

additionally contribute to CaMKIIδ activation[45] and positioning. These possibilities merit investigation in future work.

As described above, our AKAP18 knockdown and knockout findings (Figure 4e, h) suggest that there is an alternative anchor that maintains CaMKIIδ near Z-lines, from which CaMKIIδ may phosphorylate RyRs. Such redundancy is supported by previous work showing that cardiomyocytes from another murine AKAP18 (AKAP7) KO model responded normally to β-AR stimulation[50], although AKAP18δ has been shown to anchor PKA at PLN and coordinate PKA-mediated PLN phosphorylation[51]. While AKAP18δ could also serve as a PKA regulator at RyR, our preliminary work showed that Ser2808 phosphorylation during Iso treatment is maintained following AKAP18-KD (Figure S8e), further supporting the possible existence of alternative CaMKIIδ/PKA anchors. Future work will be aimed at untangling what appears to be multiple mechanisms by which CaMKIIδ and PKA regulate RyR activity.

Although the present work was focused on CaMKIIδ regulation of RyRs, it should be noted that AKAP18δ-bound CaMKIIδ additionally regulates PLN, and thus Ca^{2+} reuptake by SERCA2[16]. Since a pool of PLN protein is localized near the Z-lines[52], it is plausible that CaMKIIδ translocation during β-AR stimulation may also facilitate PLN phosphorylation at Thr17. In supplementary work, we investigated the effects of AKAP18-KD (96h, ~60 % reduction) on pThr17 and did not observe significant changes following Iso treatment in comparison with scrambled controls (Figure S8d), This lack of effect could reflect the remaining amount of AKAP18δ (~40 %) following KD. Notably, AKAP18-KD did not diminish PKA-dependent phosphorylation of Ser16 either (Figure S8f). Thus, it remains as yet unclear whether CaMKIIδ translocation is important or not for PLN regulation.

4.5 Comparison with pacing-induced CaMKIIδ translocation, and the role of microtubules

Interestingly, we found that the directionality of Iso- and 8-CPT-induced CaMKIIδ translocation was opposite from the effect of electrical pacing observed by Wood *et al*[20]. We presently confirmed this movement away from Z-lines during pacing using 2-colour dSTORM imaging, but also observed that Iso stimulation partly prevented this translocation (Figure S4b, Table S4). How do these two different stimuli have distinct effects on CaMKIIδ positioning? Wood *et al*

proposed that the pacing effects resulted from the kinase being released from binding sites at the Z-lines, allowing it to reach target sites further into the sarcomere. Could Iso stimulation counter these effects by "trapping" CaMKIIδ at the Z-lines? Support for this view comes from previous work conducted in neuronal cells, which has shown that CaMKII translocation holds the kinase at target sites following autophosphorylation[19]. In cardiomyocytes, such stickiness might reflect the larger size of the open, autophosphorylated configuration of the kinase, which could impede its drift from the tight confines of the dyad.–Since CaMKIIδ autophosphorylation occurs mainly during β-AR stimulation, but not during the weaker stimulus of electrical pacing[53], we expect that during the physiological fight-or-flight response, CaMKIIδ "trapping" at the Z-line might mitigate the effect of pacing on its movement. The true fight-or-flight response, however, includes an increase in the pacing frequency, which has not been investigated in this study, but should be examined in future investigations.

Some caution should be taken in interpreting of our microtubule disruption experiments. While it is well established that microtubules facilitate cellular transportation[54], microtubule disruption has previously been shown to affect both the structural integrity of the SR[55] and Ca^{2+} signalling in cardiomyocytes[56]. Such changes could affect CaMKIIδ translocation following Iso stimulation, such as observed in Figure 5a-d, or potentially affect the β-adrenergic signalling pathway at the dyad. Although assessment of the placement of RyR and AKAP18δ with confocal microscopy following microtubule disruption did not reveal macroscale repositioning of these proteins (Figure S10), we cannot exclude that nanoscale alterations take place near the dyad, which inhibit CaMKIIδ translocation.

Regardless of the precise underlying mechanism, distinct CaMKIIδ translocation during pacing and Iso may reflect the need to prioritize phosphorylation of Z-line RyRs during the high physiological demand associated with β-AR stimulation.

4.6 Comparison of the effects of acute and prolonged β-adrenergic stimulation

While our study has focused on the acute effects of β-AR signalling, it is well established that this signalling becomes attenuated following prolonged stimulation[11,57]. Our preliminary data indicate that changes in CaMKIIδ localization may contribute to this attenuation. In cardiomyocytes exposed to a long duration (60 min) of β-AR stimulation, we observed that the

NND from α-actinin to CaMKIIδ was no longer reduced (Figure S13a). In fact, these values tended to be higher than those observed under basal conditions. Since β-AR desensitization involves internalization and downregulation of G protein-coupled receptors[57], this retreat of CaMKIIδ from the Z-line may reflect diminishing activity of the kinase. Functionally, we have previously observed declining RyR phosphorylation during this same timeline, supporting that there is a tightly regulated system in place to counter the pro-arrhythmic effects of prolonged β-AR stimulation[11].

5. Conclusion

In summary, our findings support the view that while CaMKIIδ is highly mobile in cardiomyocytes, kinase positioning is under tight, nanoscale control. In the case of β-AR stimulation, we show that CaMKIIδ precisely translocates to the RyR nanodomain in a manner which is dependent on kinase activation, the CaMKIIδ anchor AKAP18δ, and an intact microtubular network. While further work is required to unravel the array of signalling pathways that appears to control RyR phosphorylation and CaMKIIδ, our work suggests that spatially-sensitive regulation of channel activity may fine-tune cardiomyocyte contractility to meet physiological demand. Based on our data, we suggest that targeting CaMKIIδ localization within the RyR nanodomain could provide a novel approach to correcting the channel's aberrant activity in cardiac disease.

ARTICLE INFORMATION

Funding

We are grateful for the generous financial support received from the South-Eastern Norway Regional Health Authority (A.B.D., X.S, W.E.L., under project 2020054), the Norwegian Research Council (A.B., O.M., X.S., W.E.L., under project No. 287395) and the US National Institutes of Health (D.M.B. R01HL092097, D.M.B. and J.B., R01HL142282). We also thank the Deutsche Forschungsgemeinschaft (E.K., KL1415/14-1; V.N., NI 1301/8-1) and the Else Kröner-Fresenius-Stiftung (E.K., 2023_EKSE.69).

Author contributions

Study design was conducted by A.B.D., C.R.C., X.S. and W.E.L.

A.B.D., H.S., A.B., J.L., A.H., M.L., H.U., O.M., J.B. and X.S. contributed to data acquisition. A.B.D., A.H., H.U. and X.S. contributed to data analysis. A.B.D., C.R.C., M.L., E.K., J.B., D.M.B., V.O.N., W.E.L. and X.S. contributed with interpretation. All authors contributed to the drafting and/or critical revision of the work and final approval of the work.

Acknowledgements

We thank the Section for Comparative Medicine at Oslo University Hospital Ullevål (Oslo, Norway) for expert animal care, and Per Andreas Norseng and the Core Facility for Advanced Light Microscopy for technical assistance with cellular imaging.

Conflict of interest

The other authors declare no competing interests.

References

1. Bers DM. Cardiac excitation–contraction coupling. *Nature* 2002;**415**:198-205.
2. Eisner DA, Caldwell JL, Kistamás K, Trafford AW. Calcium and Excitation-Contraction Coupling in the Heart. *Circulation Research* 2017;**121**:181-195.
3. Maier LS, Bers DM. Role of Ca^{2+}/calmodulin-dependent protein kinase (CaMK) in excitation–contraction coupling in the heart. *Cardiovascular Research* 2007;**73**:631-640.
4. Rosenberg OS, Deindl S, Sung R-J, Nairn AC, Kuriyan J. Structure of the autoinhibited kinase domain of CaMKII and SAXS analysis of the holoenzyme. *Cell* 2005;**123**:849-860.
5. Hudmon A, Schulman H. Structure-function of the multifunctional Ca^{2+}/calmodulin-dependent protein kinase II. *Biochemical Journal* 2002;**364**:593-611.
6. Couchonnal LF, Anderson ME. The Role of Calmodulin Kinase II in Myocardial Physiology and Disease. *Physiology* 2008;**23**:151-159.
7. Wehrens XHT, Lehnart SE, Reiken SR, Marks AR. Ca^{2+}/Calmodulin-Dependent Protein Kinase II Phosphorylation Regulates the Cardiac Ryanodine Receptor. *Circulation Research* 2004;**94**:e61-e70.
8. Witcher DR, Kovacs RJ, Schulman H, Cefali DC, Jones LR. Unique phosphorylation site on the cardiac ryanodine receptor regulates calcium channel activity. *Journal of Biological Chemistry* 1991;**266**:11144-11152.
9. Maier LS, Zhang T, Chen L, DeSantiago J, Brown JH, Bers DM. Transgenic CaMKIIδ_C Overexpression Uniquely Alters Cardiac Myocyte Ca^{2+} Handling. *Circulation Research* 2003;**92**:904-911.
10. Zhang T, Maier LS, Dalton ND, Miyamoto S, Ross J, Jr., Bers DM, Brown JH. The δ_C isoform of CaMKII is activated in cardiac hypertrophy and induces dilated cardiomyopathy and heart failure. *Circulation Research* 2003;**92**:912-919.

11. Shen X, van den Brink J, Bergan-Dahl A, Kolstad TR, Norden ES, Hou Y, Laasmaa M, Aguilar-Sanchez Y, Quick AP, Espe EKS, Sjaastad I, Wehrens XHT, Edwards AG, Soeller C, Louch WE. Prolonged β-adrenergic stimulation disperses ryanodine receptor clusters in cardiomyocytes and has implications for heart failure. *eLife* 2022;**11**:e77725.
12. Kolstad TR, van den Brink J, MacQuaide N, Lunde PK, Frisk M, Aronsen JM, Norden ES, Cataliotti A, Sjaastad I, Sejersted OM, Edwards AG, Lines GT, Louch WE. Ryanodine receptor dispersion disrupts Ca^{2+} release in failing cardiac myocytes. *Elife* 2018;**7**.
13. Oort RJv, McCauley MD, Dixit SS, Pereira L, Yang Y, Respress JL, Wang Q, Almeida ACD, Skapura DG, Anderson ME, Bers DM, Wehrens XHT. Ryanodine Receptor Phosphorylation by Calcium/Calmodulin-Dependent Protein Kinase II Promotes Life-Threatening Ventricular Arrhythmias in Mice With Heart Failure. *Circulation* 2010;**122**:2669-2679.
14. Curran J, Brown KH, Santiago DJ, Pogwizd S, Bers DM, Shannon TR. Spontaneous Ca waves in ventricular myocytes from failing hearts depend on Ca^{2+}-calmodulin-dependent protein kinase II. *Journal of Molecular and Cellular Cardiology* 2010;**49**:25-32.
15. Andersson DC, Marks AR. Fixing ryanodine receptor Ca^{2+} leak - a novel therapeutic strategy for contractile failure in heart and skeletal muscle. *Drug Discov Today Dis Mech* 2010;**7**:e151-e157.
16. Carlson CR, Aronsen JM, Bergan-Dahl A, Moutty MC, Lunde M, Lunde PK, Jarstadmarken H, Wanichawan P, Pereira L, Kolstad TRS, Dalhus B, Subramanian H, Hille S, Christensen G, Müller OJ, Nikolaev V, Bers DM, Sjaastad I, Shen X, Louch WE, Klussmann E, Sejersted OM. AKAP18δ Anchors and Regulates CaMKII Activity at Phospholamban-SERCA2 and RYR. *Circulation Research* 2022;**130**:27-44.
17. Tsui J, Inagaki M, Schulman H. Calcium/Calmodulin-dependent Protein Kinase II (CaMKII) Localization Acts in Concert with Substrate Targeting to Create Spatial Restriction for Phosphorylation. *Journal of Biological Chemistry* 2005;**280**:9210-9216.
18. Strack S, Choi S, Lovinger DM, Colbran RJ. Translocation of autophosphorylated calcium/calmodulin-dependent protein kinase II to the postsynaptic density. *Journal of Biological Chemistry* 1997;**272**:13467-13470.
19. Shen K, Teruel MN, Connor JH, Shenolikar S, Meyer T. Molecular memory by reversible translocation of calcium/calmodulin-dependent protein kinase II. *Nature Neuroscience* 2000;**3**:881-886.
20. Wood BM, Simon M, Galice S, Alim CC, Ferrero M, Pinna NN, Bers DM, Bossuyt J. Cardiac CaMKII activation promotes rapid translocation to its extra-dyadic targets. *Journal of Molecular and Cellular Cardiology* 2018;**125**:18-28.
21. Shen X, van den Brink J, Hou Y, Colli D, Le C, Kolstad TR, MacQuaide N, Carlson CR, Kekenes-Huskey PM, Edwards AG, Soeller C, Louch WE. 3D dSTORM imaging reveals novel detail of ryanodine receptor localization in rat cardiac myocytes. *The Journal of Physiology* 2019;**597**:399-418.
22. Lipsett DB, Frisk M, Aronsen JM, Nordén ES, Buonarati OR, Cataliotti A, Hell JW, Sjaastad I, Christensen G, Louch WE. Cardiomyocyte substructure reverts to an immature phenotype during heart failure. *The Journal of Physiology* 2019;**597**:1833-1853.
23. Bartos DC, Morotti S, Ginsburg KS, Grandi E, Bers DM. Quantitative analysis of the Ca(2+) -dependent regulation of delayed rectifier K(+) current I(Ks) in rabbit ventricular myocytes. *J Physiol* 2017;**595**:2253-2268.
24. Olivier N, Keller D, Rajan VS, Gönczy P, Manley S. Simple buffers for 3D STORM microscopy. *Biomedical Optics Express* 2013;**4**:885-899.
25. Laasmaa M, Karro N, Birkedal R, Vendelin M. IOCBIO Sparks detection and analysis software. *PeerJ* 2019;**7**:e6652.
26. Henn V, Edemir B, Stefan E, Wiesner B, Lorenz D, Theilig F, Schmitt R, Vossebein L, Tamma G, Beyermann M, Krause E, Herberg FW, Valenti G, Bachmann S, Rosenthal W, Klussmann E. Identification of a Novel A-kinase Anchoring Protein 18 Isoform and Evidence for Its Role in the

Vasopressin-induced Aquaporin-2 Shuttle in Renal Principal Cells. *Journal of Biological Chemistry* 2004;**279**:26654-26665.

27. Jumper J, Evans R, Pritzel A, Green T, Figurnov M, Ronneberger O, Tunyasuvunakool K, Bates R, Žídek A, Potapenko A, Bridgland A, Meyer C, Kohl SAA, Ballard AJ, Cowie A, Romera-Paredes B, Nikolov S, Jain R, Adler J, Back T, Petersen S, Reiman D, Clancy E, Zielinski M, Steinegger M, Pacholska M, Berghammer T, Bodenstein S, Silver D, Vinyals O, Senior AW, Kavukcuoglu K, Kohli P, Hassabis D. Highly accurate protein structure prediction with AlphaFold. *Nature* 2021;**596**:583-589.
28. Varadi M, Bertoni D, Magana P, Paramval U, Pidruchna I, Radhakrishnan M, Tsenkov M, Nair S, Mirdita M, Yeo J, Kovalevskiy O, Tunyasuvunakool K, Laydon A, Žídek A, Tomlinson H, Hariharan D, Abrahamson J, Green T, Jumper J, Birney E, Steinegger M, Hassabis D, Velankar S. AlphaFold Protein Structure Database in 2024: providing structure coverage for over 214 million protein sequences. *Nucleic Acids Research* 2023;**52**:D368-D375.
29. Rose AS, Bradley AR, Valasatava Y, Duarte JM, Prlić A, Rose PW. NGL viewer: web-based molecular graphics for large complexes. *Bioinformatics* 2018;**34**:3755-3758.
30. Rose AS, Hildebrand PW. NGL Viewer: a web application for molecular visualization. *Nucleic Acids Res* 2015;**43**:W576-579.
31. R-Core-Team. R: A Language and Environment for Statistical Computing_. R Foundation for Statistical Computing, Vienna, Austria. <https://www.R-project.org/>. 2024.
32. Posit-team. RStudio: Integrated Development Environment for R. Posit Software, PBC, Boston, MA. URL http://www.posit.co/. 2024.
33. Pereira L, Bare DJ, Galice S, Shannon TR, Bers DM. β-Adrenergic induced SR Ca^{2+} leak is mediated by an Epac-NOS pathway. *Journal of Molecular and Cellular Cardiology* 2017;**108**:8-16.
34. Grimm M, Brown JH. β-adrenergic receptor signaling in the heart: role of CaMKII. *Journal of Molecular and Cellular Cardiology* 2010;**48**:322-330.
35. Guo T, Zhang T, Mestril R, Bers DM. Ca^{2+}/Calmodulin-Dependent Protein Kinase II Phosphorylation of Ryanodine Receptor Does Affect Calcium Sparks in Mouse Ventricular Myocytes. *Circulation Research* 2006;**99**:398-406.
36. Erickson JR, Joiner ML, Guan X, Kutschke W, Yang J, Oddis CV, Bartlett RK, Lowe JS, O'Donnell SE, Aykin-Burns N, Zimmerman MC, Zimmerman K, Ham AJ, Weiss RM, Spitz DR, Shea MA, Colbran RJ, Mohler PJ, Anderson ME. A dynamic pathway for calcium-independent activation of CaMKII by methionine oxidation. *Cell* 2008;**133**:462-474.
37. Ai X, Curran JW, Shannon TR, Bers DM, Pogwizd SM. Ca^{2+}/Calmodulin-Dependent Protein Kinase Modulates Cardiac Ryanodine Receptor Phosphorylation and Sarcoplasmic Reticulum Ca^{2+} Leak in Heart Failure. *Circulation Research* 2005;**97**:1314-1322.
38. Lemieux M, Labrecque S, Tardif C, Labrie-Dion É, LeBel É, De Koninck P. Translocation of CaMKII to dendritic microtubules supports the plasticity of local synapses. *Journal of Cell Biology* 2012;**198**:1055-1073.
39. Haji-Ghassemi O, Yuchi Z, Van Petegem F. The Cardiac Ryanodine Receptor Phosphorylation Hotspot Embraces PKA in a Phosphorylation-Dependent Manner. *Molecular Cell* 2019;**75**:39-52.e34.
40. Wheeler Damian G, Groth Rachel D, Ma H, Barrett Curtis F, Owen Scott F, Safa P, Tsien Richard W. Ca(V)1 and Ca(V)2 Channels Engage Distinct Modes of $Ca(^{2+})$ Signaling to Control CREB-Dependent Gene Expression. *Cell* 2012;**149**:1112-1124.
41. Hui X, Reither G, Kaestner L, Lipp P. Targeted activation of conventional and novel protein kinases C through differential translocation patterns. *Molecular and Cellular Biology* 2014;**34**:2370-2381.
42. Tillo SE, Xiong WH, Takahashi M, Miao S, Andrade AL, Fortin DA, Yang G, Qin M, Smoody BF, Stork PJS, Zhong H. Liberated PKA Catalytic Subunits Associate with the Membrane via

Myristoylation to Preferentially Phosphorylate Membrane Substrates. *Cell Reports* 2017;**19**:617-629.

43. Shannon TR, Bare DJ, Van Dijk S, Raofi S, Huynh TN, Xiang YK, Bossuyt J, Dodge-Kafka KL, Ginsburg KS, Bers DM. Subcellular Propagation of Cardiomyocyte β-Adrenergic Activation of Calcium Uptake Involves Internal β-Receptors and AKAP7. *Function* 2022;**3**:zqac020.
44. Subramanian H, Nikolaev VO. A-Kinase Anchoring Proteins in Cardiac Myocytes and Their Roles in Regulating Calcium Cycling. *Cells* 2023;**12**:436.
45. Hudmon A, Schulman H, Kim J, Maltez JM, Tsien RW, Pitt GS. CaMKII tethers to L-type Ca^{2+} channels, establishing a local and dedicated integrator of Ca^{2+} signals for facilitation. *Journal of Cell Biology* 2005;**171**:537-547.
46. Singh P, Salih M, Tuana BS. α-kinase anchoring protein αKAP interacts with SERCA2A to spatially position Ca^{2+}/calmodulin-dependent protein kinase II and modulate phospholamban phosphorylation. *Journal of Biological Chemistry* 2009;**284**:28212-28221.
47. Johnson KR, Nicodemus-Johnson J, Carnegie GK, Danziger RS. Molecular evolution of a-kinase anchoring protein (AKAP)-7: implications in comparative PKA compartmentalization. *BMC Evolutionary Biology* 2012;**12**:125.
48. Smith FD, Reichow SL, Esseltine JL, Shi D, Langeberg LK, Scott JD, Gonen T. Intrinsic disorder within an AKAP-protein kinase A complex guides local substrate phosphorylation. *eLife* 2013;**2**:e01319.
49. Myers JB, Zaegel V, Coultrap SJ, Miller AP, Bayer KU, Reichow SL. The CaMKII holoenzyme structure in activation-competent conformations. *Nature Communications* 2017;**8**:15742.
50. Jones BW, Brunet S, Gilbert ML, Nichols CB, Su T, Westenbroek RE, Scott JD, Catterall WA, McKnight GS. Cardiomyocytes from AKAP7 knockout mice respond normally to adrenergic stimulation. *Proceedings of the National Academy of Sciences* 2012;**109**:17099-17104.
51. Lygren B, Carlson CR, Santamaria K, Lissandron V, McSorley T, Litzenberg J, Lorenz D, Wiesner B, Rosenthal W, Zaccolo M, Taskén K, Klussmann E. AKAP complex regulates Ca^{2+} re-uptake into heart sarcoplasmic reticulum. *EMBO Reports* 2007;**8**:1061-1067.
52. Wu AZ, Xu D, Yang N, Lin S-F, Chen P-S, Cala SE, Chen Z. Phospholamban is concentrated in the nuclear envelope of cardiomyocytes and involved in perinuclear/nuclear calcium handling. *Journal of Molecular and Cellular Cardiology* 2016;**100**:1-8.
53. Erickson JR, Patel R, Ferguson A, Bossuyt J, Bers DM. Fluorescence Resonance Energy Transfer–Based Sensor Camui Provides New Insight Into Mechanisms of Calcium/Calmodulin-Dependent Protein Kinase II Activation in Intact Cardiomyocytes. *Circulation Research* 2011;**109**:729-738.
54. Caporizzo MA, Prosser BL. The microtubule cytoskeleton in cardiac mechanics and heart failure. *Nature Reviews Cardiology* 2022;**19**:364-378.
55. Vega AL, Yuan C, Votaw VS, Santana LF. Dynamic changes in sarcoplasmic reticulum structure in ventricular myocytes. *J Biomed Biotechnol* 2011;**2011**:382586.
56. Gómez AM, Kerfant BG, Vassort G. Microtubule Disruption Modulates Ca^{2+} Signaling in Rat Cardiac Myocytes. *Circulation Research* 2000;**86**:30-36.
57. Kayki-Mutlu G, Koch WJ. Nitric Oxide and S-Nitrosylation in Cardiac Regulation: G Protein-Coupled Receptor Kinase-2 and β-Arrestins as Targets. *International Journal of Molecular Sciences* 2021;**22**.

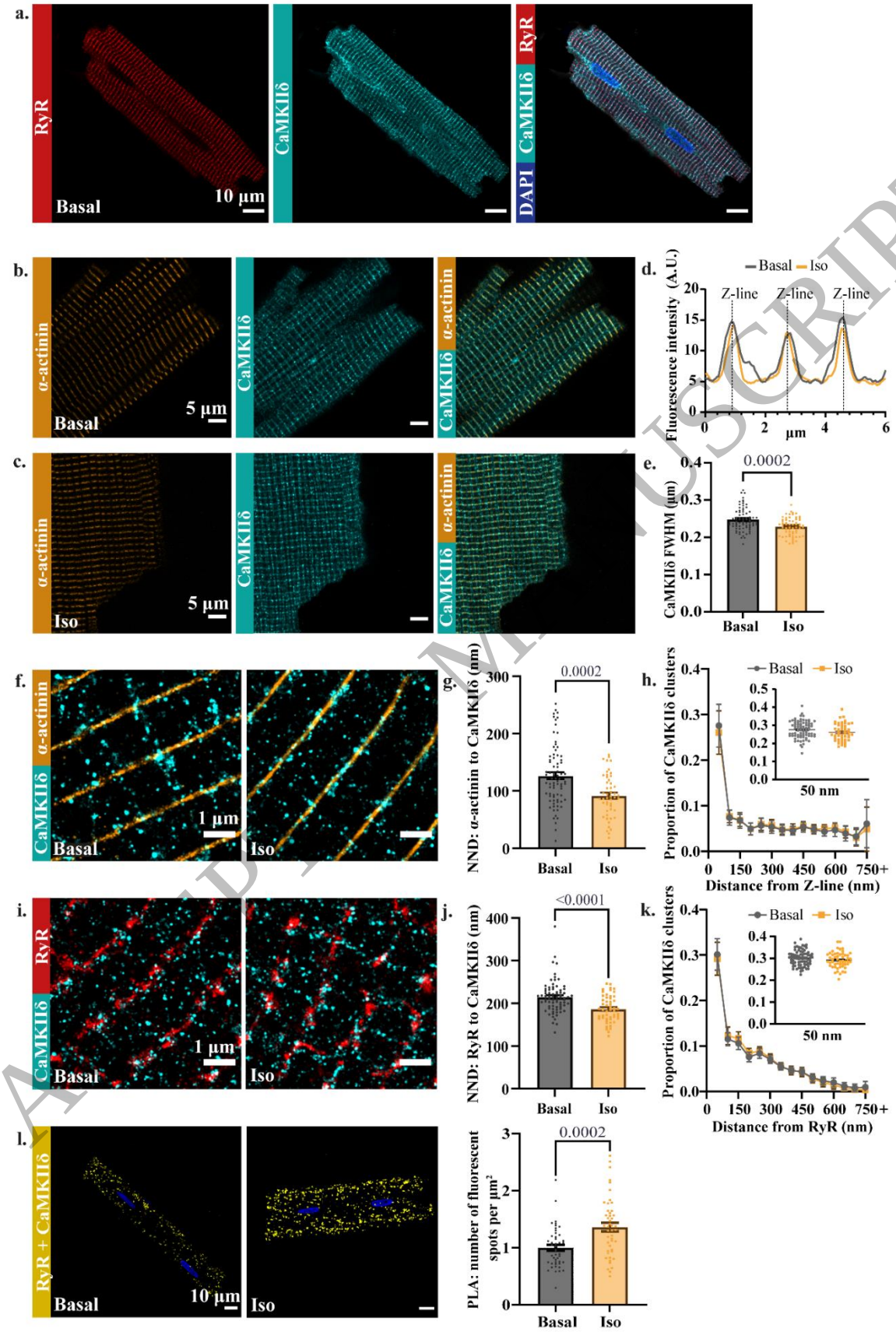

1 **Figure 1: β-adrenergic stimulation promotes Ca^{2+}/Calmodulin-dependent kinase IIδ (CaMKIIδ)**

translocation towards the ryanodine receptor (RyR) nanodomain.

(a) Representative immunofluorescence images of RyR (red), CaMKIIδ (cyan) and an overlay with DAPI (blue) in isolated rat cardiomyocytes. **(b-c)** Representative images of α-actinin (orange), CaMKIIδ (cyan) and an overlay at **(b)** baseline and **(c)** following isoproterenol (Iso, 100 nM, 10 min). **(d)** Representative fluorescence intensity profile of CaMKIIδ from cardiomyocytes with basal (grey) or Iso treatment (yellow). **(e)** Quantification of Full-Width-Half-Maximum (FWHM) from CaMKIIδ fluorescence peaks corresponding to α-actinin fluorescence peaks. Statistical differences examined by nested ANOVA (basal: $n_{hearts} = 10$, $n_{cells} = 78$, Iso: $n_{hearts} = 11$, $n_{cells} = 63$). **(f)** Representative 2-colour 2D-dSTORM images of cardiomyocyte labelled with α-actinin (orange) and CaMKIIδ (cyan) ± Iso. **(g)** Average nearest neighbour distance (NND) from α-actinin to CaMKIIδ. **(h)** CaMKIIδ cluster proportions found within 50 nm increments from Z-line (α-actinin). Inset: Individual data points for clusters within 50 nm. **(i)** Representative 2-colour dSTORM images of cardiomyocyte labelled with RyR (red) and CaMKIIδ (cyan). **(j)** Average NND from RyR to CaMKIIδ. **(k)** CaMKIIδ cluster proportions found within 50 nm increments from RyR. Inset: Individual data points for clusters within 50 nm. Statistical differences examined by **(g, j)** Mann-Whitney test or **(h, k)** two-way-ANOVA (see table S1, S2) (**g,h**: basal: $n_{hearts} = 13$, $n_{cells} = 78$, Iso: $n_{hearts} = 10$, $n_{cells} = 49$, **j, k**: basal: $n_{hearts} = 10$, $n_{cells} = 75$, Iso: $n_{hearts} = 10$, $n_{cells} = 52$). **(l)** Representative confocal images of proximity ligation assay of RyR and CaMKIIδ (yellow) with nuclei stained by DAPI (blue). Right panel: number of fluorescent ligation events per μm^2, normalized to respective basal treatment. Statistical differences examined by Mann-Whitney test (basal: $n_{hearts} = 3$, $n_{cells} = 46$, Iso: $n_{hearts} = 3$, $n_{cells} = 47$). Bar charts present mean values ±SEM with each data point representing the mean of one cardiomyocyte. XY-charts present mean values ±SD. Normality of distributions was confirmed by Shapiro-Wilk's test. A p-value ≤ 0.05 was considered statistically significant.

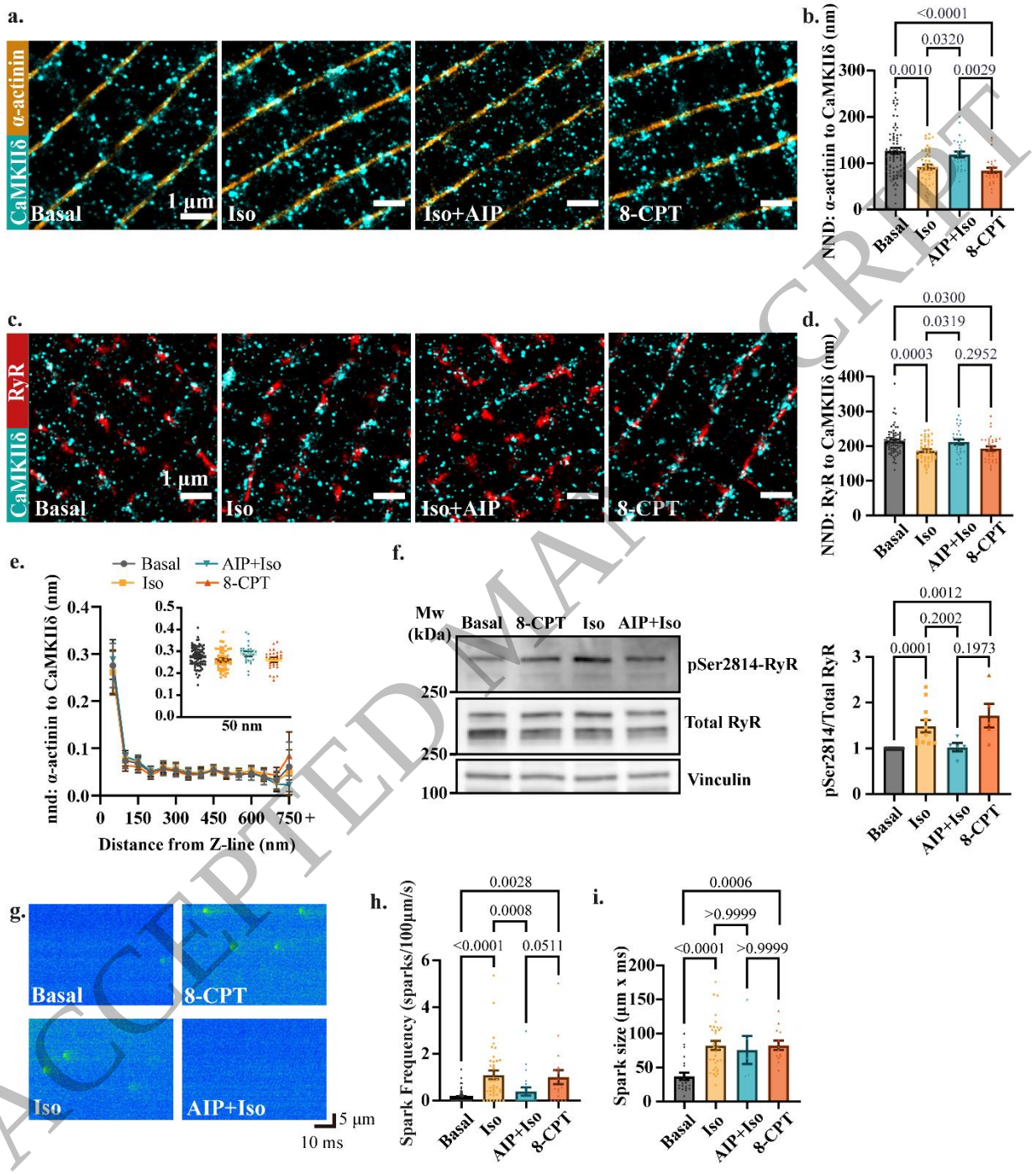

Figure 2: CaMKIIδ translocation towards the RyR nanodomain is dependent on kinase activation and is accompanied by increased RyR phosphorylation and Ca^{2+} spark frequency.
(a-d) Representative 2-colour dSTORM images of **(a)** α-actinin (orange) and CaMKIIδ (cyan), or **(c)** RyR (red) and CaMKIIδ (cyan) in isolated rat cardiomyocytes following basal treatment, isoproterenol (Iso, 100 nM, 10 min), AIP (2 µM, 45 min) treatment following Iso stimulation, or 8-CPT (10 µM, 10 min). NND from **(b)** α-actinin to CaMKIIδ or **(d)** RyR to CaMKIIδ was compared per cell. Statistical

differences were examined by Kruskal-Wallis test with Dunn's post hoc correction. **(e)** Proportion of CaMKIIδ clusters found within 50 nm increments from α-actinin clusters following basal, Iso, AIP+Iso, and 8-CPT treatment. Inset: individual data points for clusters within 50 nm of α-actinin. Statistical differences examined by a two-way-ANOVA (see table S8) (**b, e**: basal: n_{hearts} = 13, n_{cells} = 78, Iso: n_{hearts} = 10, n_{cells} = 49, AIP+Iso: n_{hearts} = 6, n_{cells} = 29, 8-CPT: n_{hearts} = 6, n_{cells} = 27, **d**: basal: n_{hearts} = 10, n_{cells} = 75, Iso: n_{hearts} = 10, n_{cells} = 52, AIP+Iso: n_{hearts} = 3, n_{cells} = 29, 8-CPT: n_{hearts} = 5, n_{cells} = 34). **(f)** Representative Western blots and quantification of the relative amount of CaMKIIδ-phosphorylated RyR (pSer2814-RyR) in cardiomyocytes following basal treatment, 8-CPT, Iso or AIP+Iso. Values were normalized to basal treatment. Statistical differences examined by Kruskal-Wallis test with Dunn's post hoc correction (basal: n_{hearts} = 11, Iso: n_{hearts} = 11, AIP+Iso: n_{hearts} = 5, 8-CPT: n_{hearts} = 5). **(g)** Representative Ca^{2+} spark recordings from Basal, Iso, 8-CPT and AIP+Iso treated cardiomyocytes, and measurements of **(h)** Ca^{2+} spark frequency and **(i)** spark size. Statistical differences examined by Kruskal-Wallis test with Dunn's post hoc correction (**h:** basal: n_{hearts} = 5, n_{cells} = 57, Iso: n_{hearts} = 6, n_{cells} = 39, AIP+Iso: n_{hearts} = 3, n_{cells} = 19, 8-CPT: n_{hearts} = 3, n_{cells} = 18, **i:** basal: n_{hearts} = 5, n_{cells} = 21, Iso: n_{hearts} = 6, n_{cells} = 33, AIP+Iso: n_{hearts} = 3, n_{cells} = 5, 8-CPT: n_{hearts} = 3, n_{cells} = 13). Bar charts present mean values ±SEM with each data point representing the mean of (**b, d, h, i**) one cardiomyocyte or (**f**) heart. XY-charts present mean values ±SD. Normality of distributions was confirmed by Shapiro-Wilk's test. A p-value ≤ 0.05 was considered statistically significant.

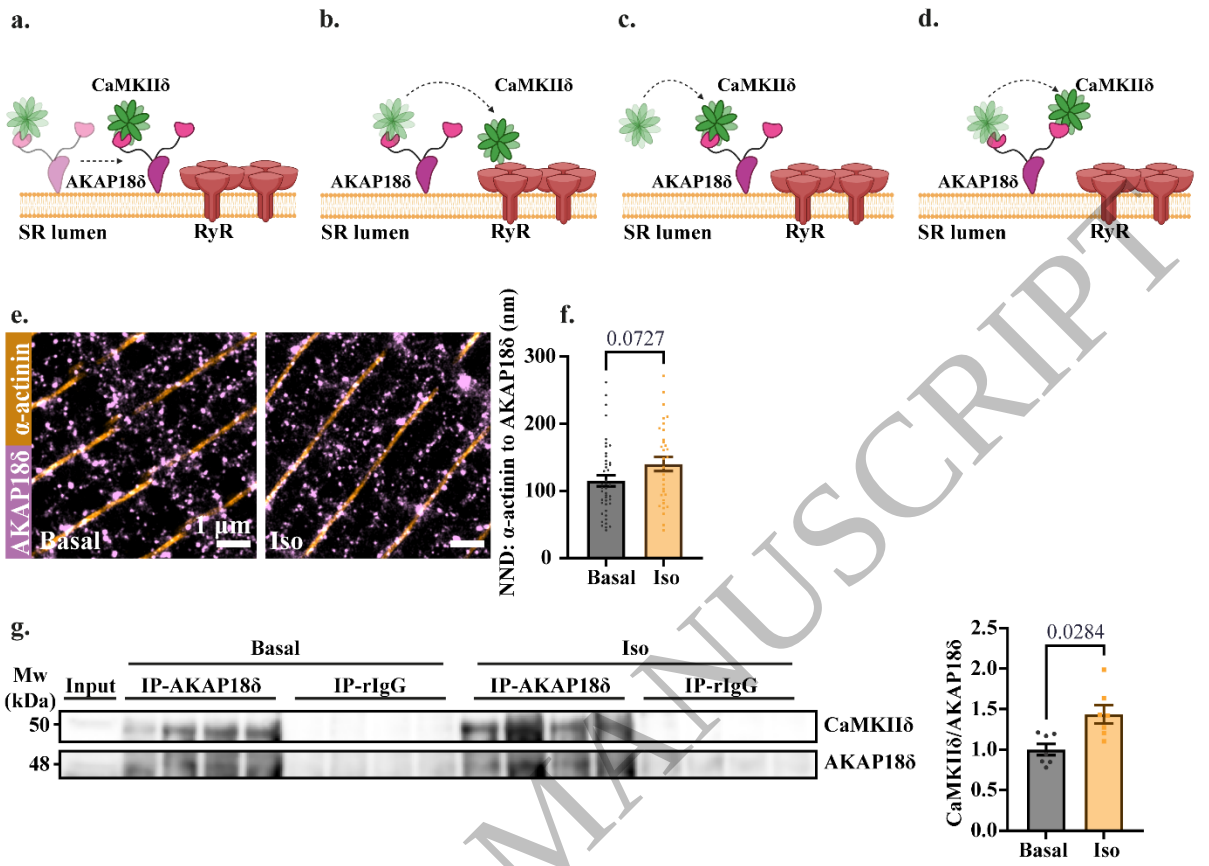

Figure 3: The role of A-kinase anchoring protein 18δ (AKAP18δ) in CaMKIIδ anchoring and translocation.

(a-d) Illustrations of potential roles of AKAP18δ in CaMKIIδ translocation following kinase activation, mediated via **(a)** movement of AKAP18δ, **(b)** release of CaMKIIδ from AKAP18δ, **(c)** recruitment of CaMKIIδ to AKAP18δ, **(d)** altered CaMKIIδ binding within AKAP18δ. Note that AKAP18δ is presented as a monomer for simplicity. The illustration displays a 1:2 stoichiometric relationship between CaMKIIδ and RyR for ease of presentation, although the true stoichiometry is not known. **(e)** Representative 2-colour dSTORM images of α-actinin (orange) and AKAP18δ (pink) from basal and Iso treated cardiomyocytes. **(f)** NND from α-actinin to AKAP18Iδ was compared per cell. Statistical differences examined by Mann-Whitney test (basal: n_{hearts} = 6, n_{cells} = 44, Iso: n_{hearts} = 6, n_{cells} = 32). **(g)** Immunoprecipitation of CaMKIIδ-AKAP18δ from basal or Iso-treated cardiomyocyte lysate. Rabbit IgG was used as a negative control. Statistical differences examined by Mann-Whitney test (basal: n_{hearts} = 7, Iso: n_{hearts} = 7). Bar charts present mean values ±SEM with each data point representing the mean of **(f)** one cardiomyocyte or **(g)** heart. Normality of distribution confirmed by Shapiro-Wilk's test. A p-value ≤ 0.05 was considered statistically significant. **(a-d)** Created with BioRender.com.

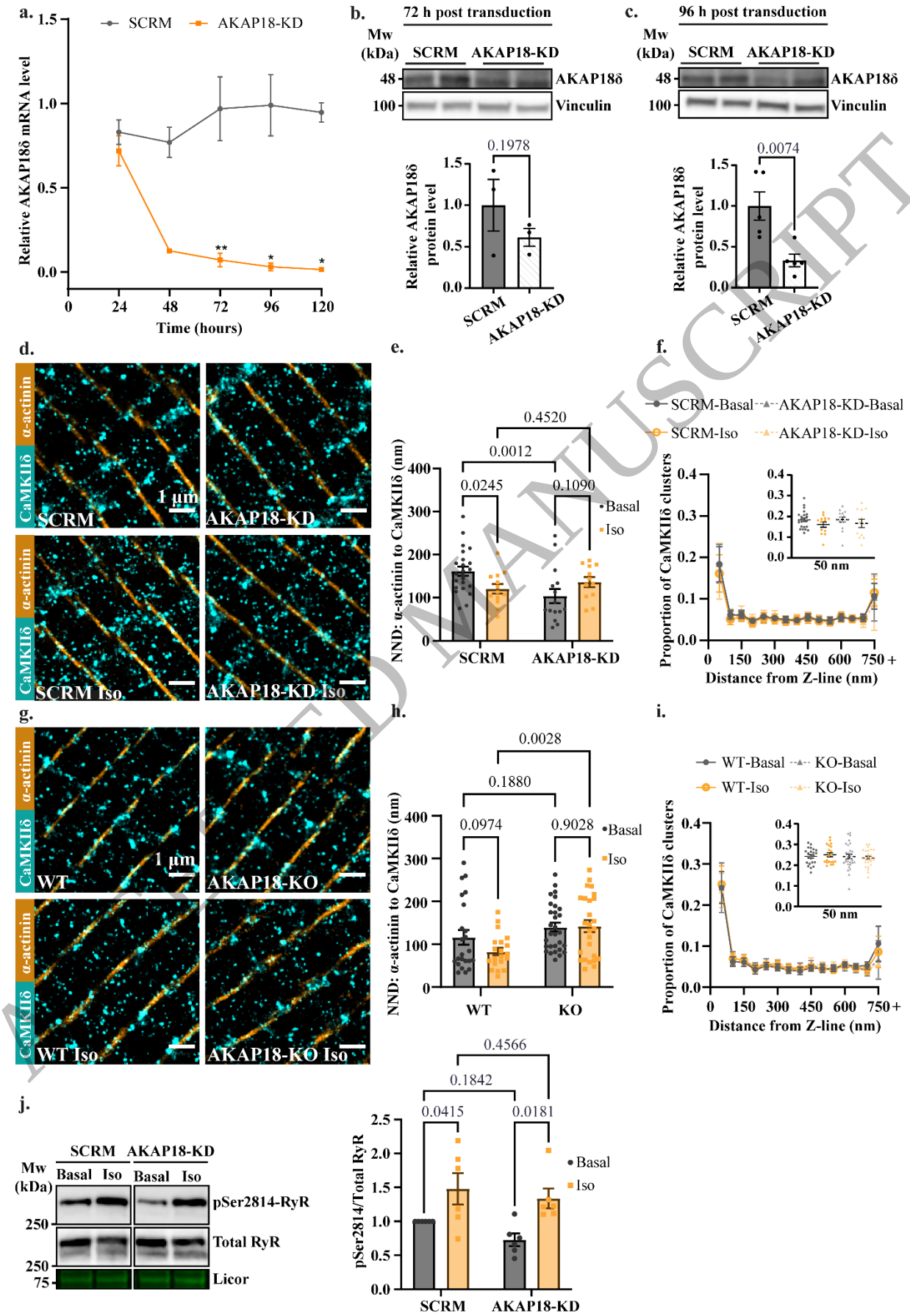

(a) mRNA expression of AKAP18 at 24 h intervals in isolated cardiomyocytes treated with adenovirus containing a scrambled control sequence or a short hairpin sequence targeting AKAP18. Statistical differences examined by Paired Student's t-test (* $p < 0.05$, ** $p < 0.01$, $n_{24h} = 2$, $n_{48h} = 2$, $n_{72h} = 4$, $n_{96h} = 7$, $n_{120h} = 2$). **(b, c)** Effect of viral AKAP18-knock-down treatment (AKAP18-KD) on protein levels compared to a scrambled control virus (SCRM) in cardiomyocytes cultured for **(b)** 72 h or **(c)** 96 h post viral transduction. Significant differences examined by paired Student's t-test (**b**: n = 3, **c**: n = 5). **(d)** Representative 2-colour dSTORM images of α-actinin (orange) and CaMKIIδ (cyan) from basal and isoproterenol (Iso, 10 min, 100 nM) treatment in rat cardiomyocytes cultured for 96 h with SCRM or AKAP18-KD virus. Effects of KD were examined on **(e)** NND from α-actinin to CaMKIIδ, and **(f)** the proportion of CaMKIIδ found within 50 nm increments of α-actinin. Inset: individual data points for clusters within 50 nm of α-actinin. **(g-i)** Representative recordings and measurements as in **(d-f)** in isolated cardiomyocytes from wild-type (WT) and AKAP18γ/δ-knockout (KO) mice. Statistical differences were examined by two-way-ANOVA, with results displayed **(e, h**: Fisher's LSD test**)** or in table S11 and S12 **(f, i)**. **(e, f**: SCRM-basal: $n_{hearts} = 7$, $n_{cells} = 23$, AKAP18-KD-basal: $n_{hearts} = 4$, $n_{cells} = 15$, SCRM-Iso: $n_{hearts} = 6$, $n_{cells} = 13$, AKAP18-KD-Iso: $n_{hearts} = 4$, $n_{cells} = 12$, **h, i**: WT-basal: n_{hearts} 4 =, $n_{cells} = 23$, KO-basal: $n_{hearts} = 5$, $n_{cells} = 30$, WT-Iso: $n_{hearts} = 4$, $n_{cells} = 20$, KO-Iso: $n_{hearts} = 5$, $n_{cells} = 26$). **(j)** Representative immunoblots and quantification of the relative amount of CaMKIIδ-phosphorylated RyR (pSer2814-RyR) in cardiomyocytes from SCRM or AKAP-KD rat cardiomyocytes treated with basal treatment or Iso. Licor was used to show equal protein loading. Values normalized to SCRM basal treatment. Statistical differences examined by a two-way ANOVA with Fisher's LSD test (n = 6). Bar charts present mean values ±SEM with each data point representing the mean of (**a, b, c, j**) from one heart or (**e, h**) cardiomyocyte. XY-charts present mean values ±SD. Normality of distributions confirmed by Shapiro-Wilk's test. A p-value ≤ 0.05 was considered statistically significant.

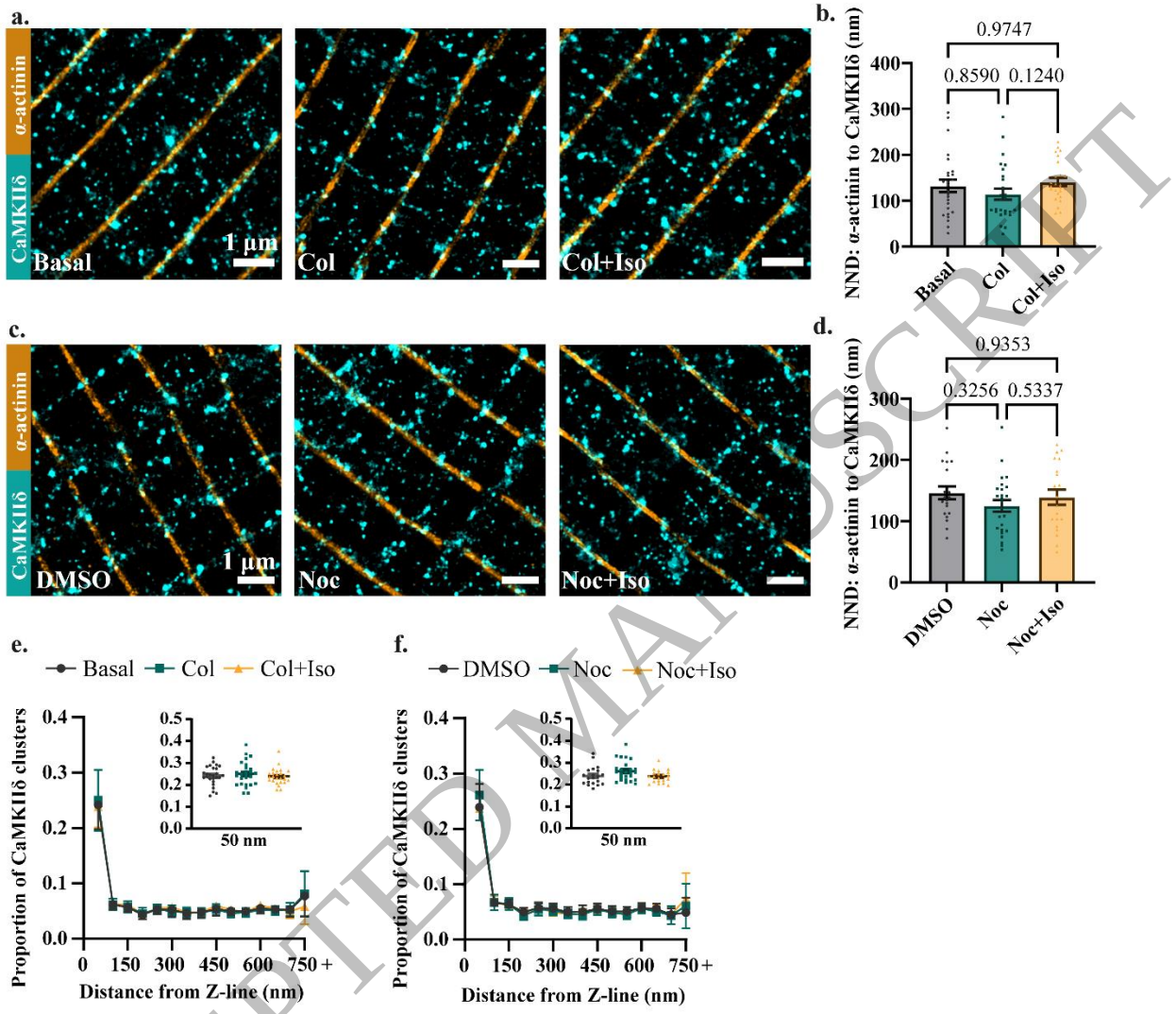

Figure 5: Microtubular destabilization inhibits Iso-dependent CaMKIIδ translocation.
(a) Representative 2-colour dSTORM images of α-actinin (orange) and CaMKIIδ (cyan) in isolated cardiomyocytes treated with basal treatment or colchicine (Col, 10 µM, 2 h) ± Isoproterenol (Iso, 100 nM, 10 min). **(b)** Effects on NND from α-actinin to CaMKIIδ. **(c, d)** Representative recordings and measurements as in **(a, b)** in cells treated with basal treatment w DMSO (DMSO) or nocodazole (Noc, 10 µM, 2h) ± Iso (Noc+Iso). Significant differences examined by Kruskal-Wallis with Dunn's post hoc comparisons. **(e, f)** Proportion of CaMKIIδ clusters found within 50 nm increments from α-actinin clusters. Inset: individual data points from clusters within 50 nm of α-actinin for **(e)** cells treated with basal treatment, Col or Col+Iso, or **(f)** cells treated with DMSO, Noc or Noc+Iso. Statistical differences examined by a two-way ANOVA (see table S13 and S14) (**b, e**: Basal: $n_{hearts} = 4$, $n_{cells} = 26$, Col: $n_{hearts} = 4$, $n_{cells} = 26$, Col+Iso: $n_{hearts} = 4$, $n_{cells} = 25$, **d, f**: DMSO: $n_{hearts} = 4$, $n_{cells} = 20$, Noc: $n_{hearts} = 4$, $n_{cells} = 25$, Noc+Iso: $n_{hearts} = 4$, $n_{cells} = 20$). Bar charts present mean values ±SEM with each data point representing

the mean of one cardiomyocyte. XY-charts present mean values ±SD. Normality of distribution confirmed by Shapiro-Wilk's test. A p-value ≤ 0.05 was considered statistically significant.

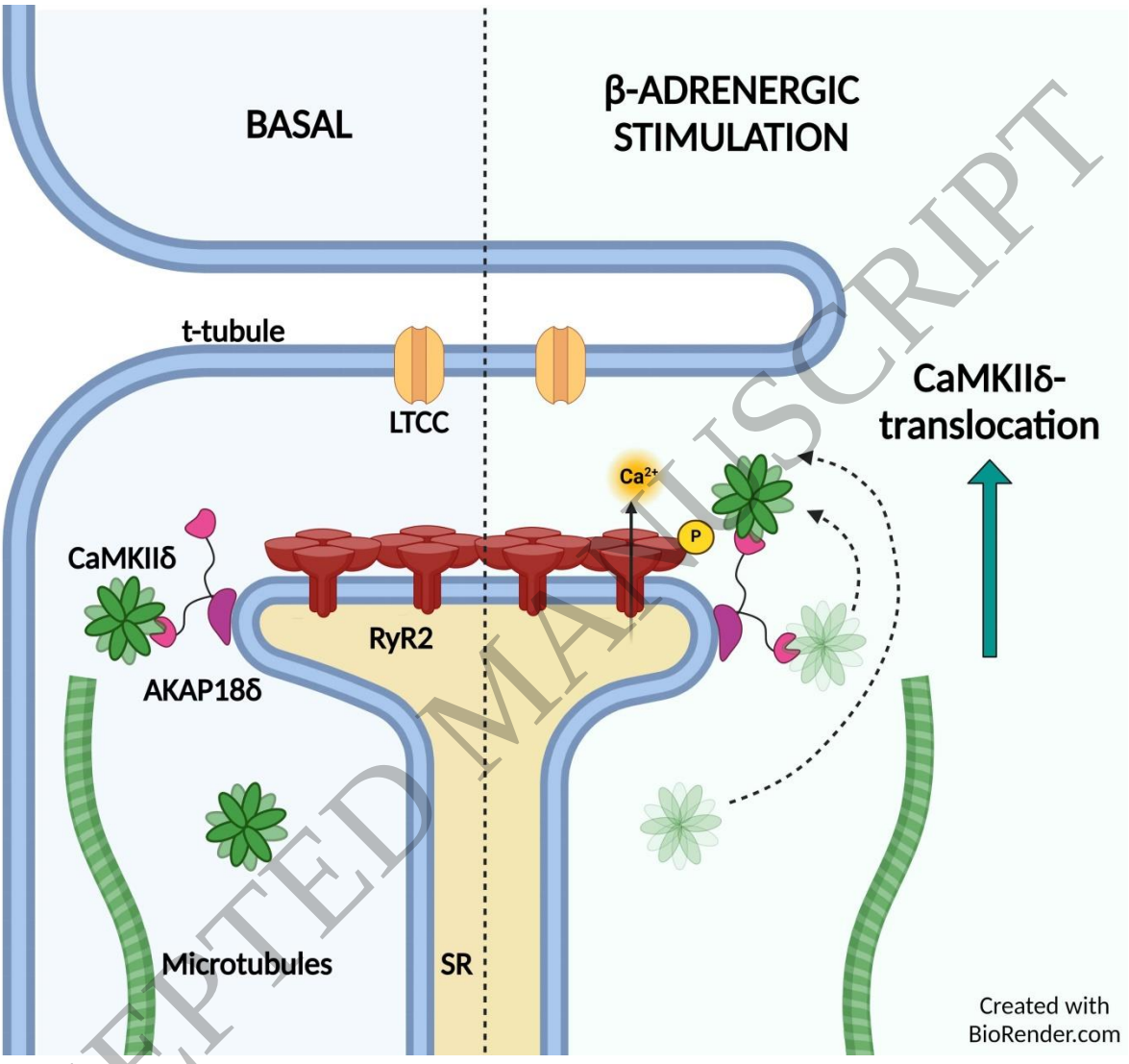

Graphical Abstract
559x489 mm (x DPI)